Annales Geophysicae, 23, 3451–3455, 2005
SRef-ID: 1432-0576/ag/2005-23-3451

Annales Geophysicae

A comparison of satellite scintillation measurements with HF radar backscatter characteristics

S. E. Milan[1], **S. Basu**[2], **T. K. Yeoman**[1], **and R. E. Sheehan**[3]

[1]Department of Physics and Astronomy, University of Leicester, Leicester LE1 7RH, UK
[2]Space Vehicles Directorate, Air Force Research Laboratory, Hanscom Air Force Base, Masachusetts 01731, USA
[3]Institute for Scientific Research, Boston College, Newton Center, Massachusetts 02467, USA

Received: 1 July 2005 – Revised: 15 September 2005 – Accepted: 11 October 2005 – Published: 21 December 2005

Abstract. We examine the correspondence between high latitude ionospheric scintillation measurements made at 250 MHz with the occurrence of 10 MHz HF coherent radar backscatter, on 13 and 14 December 2002. We demonstrate that when the ionospheric intersection point of the scintillation measurements is co-located with significant HF radar backscatter, the observed scintillation, quantified by the S4 index, is elevated. Conversely, when the radar indicates that backscatter is observed away from the intersection point due to movements of the auroral zone, the observed scintillation is low. This suggests that scintillation is highly location-dependent, being enhanced in the auroral zone and being lower at sub-auroral latitudes. The coexistence of scintillation and HF radar backscatter, produced by ionospheric density perturbations with scale sizes of 100 s of metres and ∼15 m, respectively, suggests that a broad spectrum of density fluctuations is found in the auroral zone.

Keywords. Ionosphere (Auroral ionosphere; Ionospheric irregularities) – Radio science (Space and satellite communication)

1 Introduction

Signal power fluctuations in trans-ionospheric satellite transmissions, known as ionospheric scintillation, are predominantly produced by forward scatter of the radio waves by ionospheric irregularities in the electron density at F region altitudes. Depending on the frequency of transmission, irregularities of different scale sizes contribute to the magnitude of scintillation. At frequencies of 250 MHz, as employed by the receiving system at Ny Ålesund, Svalbard, irregularities with wavelengths in the range of 100 m to 1 km are the major contributors to scintillation. At smaller scales, field-aligned decametre irregularities can coherently scatter HF radio waves, in a manner akin to Bragg scatter. For instance, backscatter of 10 MHz signals from 15 m irregularities in the auroral ionosphere allows the SuperDARN radar network (Greenwald et al., 1995) to investigate motions of the ionosphere under the influence of the magnetospheric electric field. Near the magnetic equator, the relationship between sub-km scale irregularities causing scintillations at VHF frequencies and 3-m irregularities causing coherent scatter at 50 MHz has been investigated (Basu et al., 1978). A hierarchy of plasma instabilities has been suggested to explain the phenomenon, in which the generation of progressively shorter wavelength modes by larger primary waves has been envisaged (Woodman and Basu, 1976). At present, the relationship between irregularities of such differing wavelengths are not known at high latitudes, in the auroral oval and the polar cap, though it is thought that short scale waves can grow in the density gradients of long scale waves or that long wavelength waves can energy-cascade to produce shorter scale length fluctuations under the influence of the $\boldsymbol{E}\times\boldsymbol{B}$ instability and velocity shear (Tsunoda, 1988; Basu et al., 1988).

In this paper we investigate the relationship between high latitude scintillation measurements, made using 250 MHz transionospheric satellite signals, with observations of ionospheric backscatter by the CUTLASS Finland radar (e.g. Milan et al., 1997), part of the SuperDARN network. In particular, we compare the backscatter power with the S4 scintillation index at 250 MHz. The S4 index is defined as the ratio of the standard deviation of signal power fluctuations divided by the average power. It can be shown that the S4 index is proportional to the column integrated electron density deviation ΔN (Basu and Basu, 1993). We perform the comparison for the 48-hour period spanning the 13 and 14 December 2002. These two days were selected for investigation as they represented a magnetically quiet day and a moderately disturbed day (daily average K_p of 1 and 3-, respectively), corresponding respectively to very weak and strong scintillation activity.

Correspondence to: S. E. Milan
(steve.milan@ion.le.ac.uk)

2 Observations

Figure 1 shows latitude-time plots of Doppler shift and backscatter power measured along beam 8 of the Finland radar, for the 13 and 14 December 2002. Intensity scintillation measurements at Ny Ålesund, Svalbard, are performed by receiving the 250 MHz signals from a quasi-stationary polar satellite (Basu et al., 1998). The satellite signal is recorded at 125 Hz and the S4 index of scintillation is computed every 65 sec. The times at which scintillation measurements at elevation angles exceeding 60° are available are indicated by bars between the two panels, labeled S4. The radar switched between two operating modes a few times during the period, as indicated by vertical dotted lines. The radar operated in its normal mode (180 km to the first gate, 45 km gates, 3 s dwell) for the intervals 00:00–06:00 UT and ∼12:00–24:00 UT on each day. Between 06:00 and ∼12:00 UT the radar operated in a 30 km range gate mode, with the range to the first gate set at 900 km; for this reason, no data is available equatorward of ∼69° latitude at these times.

Scintillation originates at F region heights and is assumed to be concentrated around 300 km, the height of maximum ionization density. During 08:00–14:00 UT, the 300 km altitude intersection point lies within the elliptical area shown in Fig. 2. While the intersection point moves with time, it is generally contained within two range cells of the radar field-of-view, gates 38 and 39 of beam 8, when the radar is operating in the 45 km range resolution mode, though we note that the radar range-finding is only accurate to the order of one range gate due to refraction effects in the ionosphere (Yeoman et al., 2001). The intersection point dwells within gate 39 for the majority of the interval, and hence we perform our comparison between scintillation and HF coherent backscatter measurements from this cell. The corresponding cell for the 30 km mode is gate 35. The average latitude of the scintillation measurements is indicated by the horizontal dashed line in Fig. 1. The radar was operating at 10 MHz throughout this interval, and therefore is sensitive to ionospheric irregularities with scale sizes of 15 m.

Backscatter echoes with low Doppler shift (generally below 50 m s^{-1}) and low spectral width (below approximately 20 m s^{-1}) are automatically identified as backscatter from the ground (see e.g. Milan et al., 1997), and are indicated in grey in panel (a) of Fig. 1. However, there is considerable ambiguity in this identification as these characteristics are also consistent with backscatter from slow-moving ionospheric irregularities. Hence, care must be exercised in discriminating between ionospheric and ground backscatter. However, we can use this identification to gain an understanding of the radar propagation characteristics. It is most important to remember that the observation of ionospheric backscatter is controlled by two factors: the presence of irregularities in the ionosphere from which to scatter, and a suitable propagation mode to allow transmission of the signals to and from the radar (see also Milan et al., 1998). Figure 3 presents a schematic representation of the backscatter observed in Fig. 1, and the propagation modes by which the backscatter is observed.

We identify sporadic scatter at latitudes below 67° as the "grainy near-range echoes" associated with scatter from meteor trails at D region altitudes (Hall et al., 1997); we will not consider these echoes further.

During the day when the high latitude ionosphere is illuminated by the sun, approximately 06:00–16:00 UT, a region of ground backscatter is observed between latitudes 67 and 75° degrees. This indicates that the F-region electron density has grown sufficiently to reflect the radar signals to the ground. These signals are then forward-scattered back into the ionosphere, allowing ionospheric backscatter to be observed from further ranges (latitudes 76° and beyond); the reader is directed to Milan et al. (1997) for a fuller description of radar propagation modes. At night the F region electron density is diminished and ground backscatter is no longer observed between 67 and 75°; instead ionospheric scatter is observed at these ranges, though some of it is misidentified as ground scatter by the automated algorithm (e.g. 00:00–06:00 UT, 68–71° latitude, 13 and 14 December) as a consequence of having low Doppler shifts. The ionospheric scatter therefore displays a diurnal variation in the range at which it is observed, 67–75° at night and 76–84° during the day. This is just the expected diurnal variation of the location of the auroral oval (e.g. Feldstein and Starkov, 1967). Superimposed on this diurnal motion are motions associated with the expansion and contraction of the polar cap: the auroral oval expands to lower latitudes during intervals of intense solar wind-magnetosphere coupling and contracts polewards during more quiescent periods (see e.g. Milan et al., 2003). As a consequence, the auroral zone appears at higher latitudes on the 13 December than on the following day. It can be seen, then, that on 13 December the auroral zone is located at slightly higher latitudes than the scintillation measurement point, and here the radar observed only sporadic and low signal power backscatter. In contrast, on 14 December, the auroral zone is located at lower latitudes, coincident with the scintillation measurement point, especially between 10:00 and 14:00 UT. We can make the first tentative assertion that little scintillation is observed on the 13 December as it is the sub-auroral ionosphere that is sampled, where few ionospheric irregularities are found (indeed where little radar backscatter is seen). In contrast, greater levels of scintillation are observed on the 14 December as the auroral zone ionosphere is sampled, where ∼15 m ionospheric irregularities abound. These observations therefore indicate a link between the occurrence of ∼1 km irregularities, which increase scintillation of 250 MHz signals, and the ∼15 m irregularities that give rise to HF radar backscatter.

A more quantitative comparison of backscatter power and the S4 index is provided in Fig. 4. The two sets of panels correspond to the 13 and 14 December, respectively. The bottom panel in each shows the S4 index. The top panels show the coherent backscatter power from the ionospheric intersection point (solid curve) and also the backscatter power of ground scatter from the ground reflection point which provides the

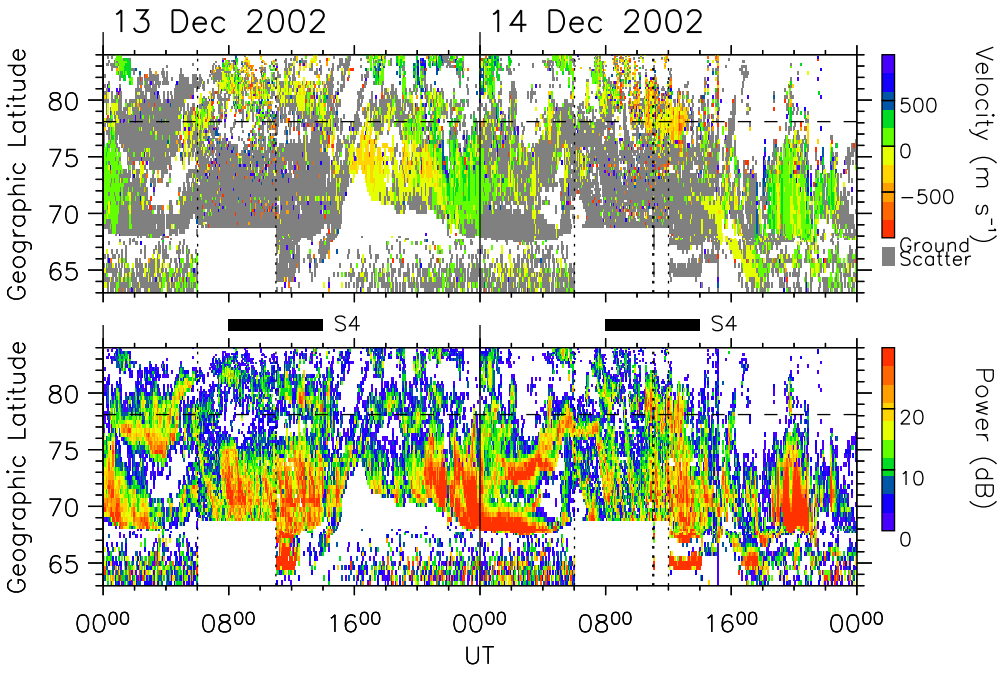

Fig. 1. Latitude-time velocity and power plots from beam 8 of the CUTLASS Finland radar on 13 and 14 December 2002. In the upper panel, backscatter identified as ground scatter is indicated in grey. Vertical dotted lines show times at which the radar changes scanning mode (see text for details). The horizontal dashed lines show the ionospheric intersection point of the satellite signals. The times that scintillation observations are available are shown by horizontal bars marked S4.

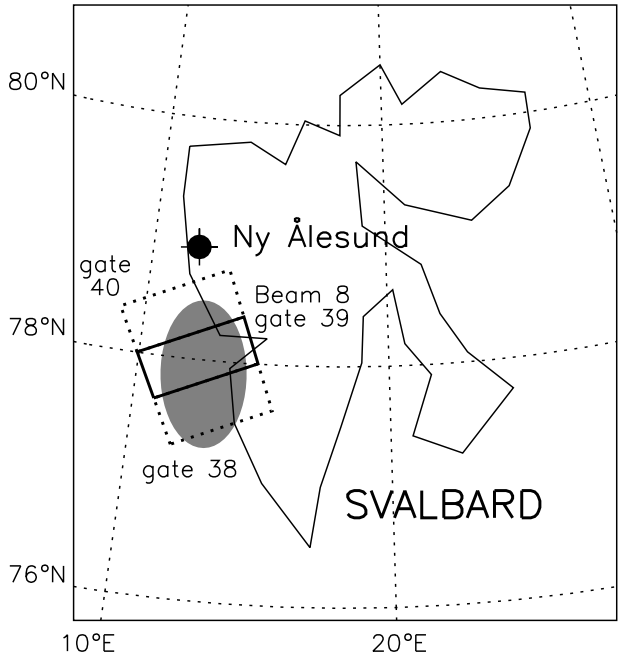

Fig. 2. (a) A map of Svalbard, showing the ground station at Ny Ålesund, the ionospheric intersection point of the scintillation measurements (grey ellipse), and the locations of gates 38, 39, and 40 of beam 8 the Finland radar.

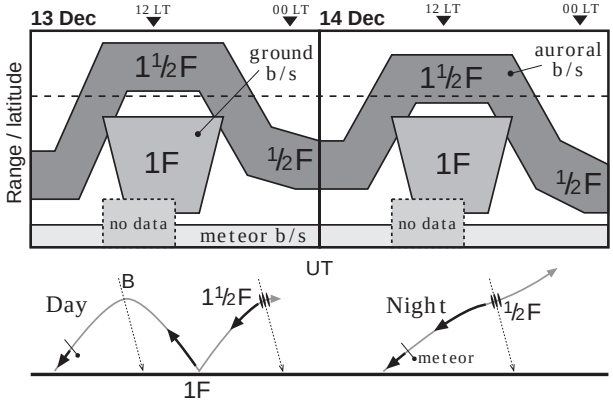

Fig. 3. A schematic indicating our interpretation of the origin of backscatter during the 13 and 14 December 2002. Also shown are the assumed propagation modes that give rise to the observed backscatter, for daytime and nighttime ionospheric conditions. Grey rays show the out-going radar signal, with black arrows showing regions of backscatter, including meteor, ground, and ionospheric backscatter. Ionospheric scatter is only observed where ∼15 m field-aligned irregularities are present.

forward-scatter for the intersection cell (dotted curve); for clarity of presentation the data have been averaged to one tenth of their original temporal resolution. These values are the power measured when the radar is operating in the 45 km mode; we add a correction factor of $+20\log_{10}(45/30)$, or

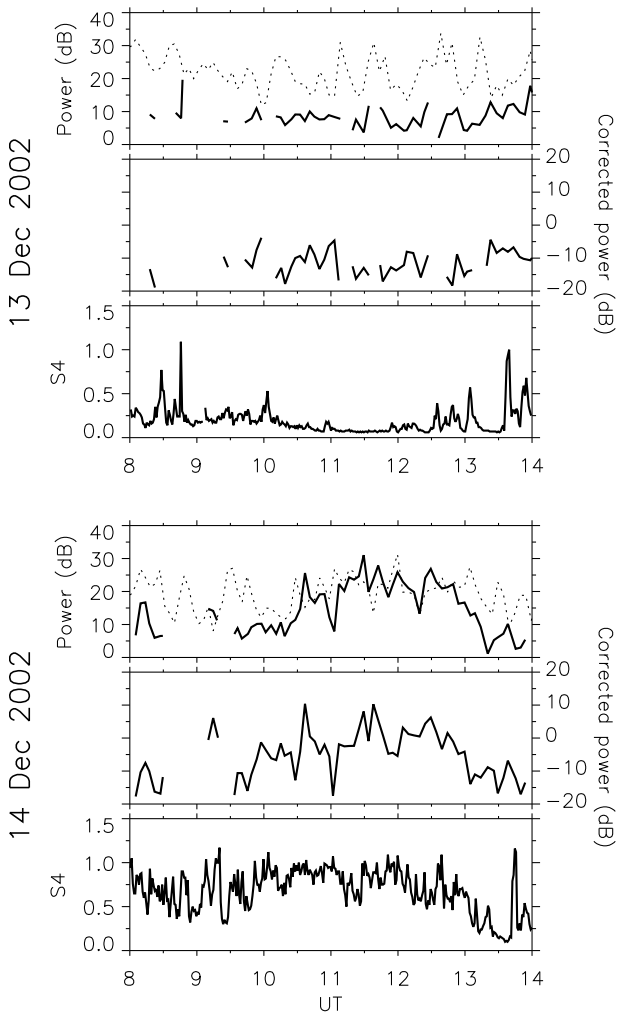

Fig. 4. A comparison of radar backscatter and scintillation measurements from the intersection point, for the 13 (top panels) and 14 (bottom panels) December 2002. In each case: (top panel) ionospheric backscatter power (solid curve) and ground scatter power from ground reflection point (dotted curve); (middle panel) corrected power (see text); (bottom panel) S4 scintillation index.

3.5 dB, when the radar is operating with 30 km range gates to account for the smaller scattering volume (see also Lester et al., 2004). We consider the solid, ionospheric scatter curves alone first. On the 13 December, auroral backscatter is observed only sporadically (this is especially apparent before averaging), and then with backscatter powers of order 10 dB. This compares with the S4 measurements which are low throughout this interval, averaging 0.2–0.5. On the 14 December, auroral backscatter is observed more consistently throughout the 6-hour interval, and has elevated backscatter powers of order 10–30 dB. Correspondingly, S4 varies between 0.5 and 1.0 during this interval.

We must also consider the possibility that the backscatter powers observed are governed not only by the backscatter cross-section of irregularities within the intersection volume, but also by factors affecting the propagation of the radar signals to and from the volume, such as focusing and defocusing of the radar signal, or absorption in the D region (e.g. Milan et al., 1999). If we assume that the ground provides a "standard candle" target for the radar, then variations in backscatter power of the ground reflection (dotted curve) will mirror the perturbation produced by propagation through the ionosphere. By subtracting the ground power from the ionospheric power we produce a "corrected power" which should more accurately reflect changes in backscatter cross-section within the intersection volume (middle panels). Now, on the 13 December, corrected powers are of the order of -10 dB, to compare with the average S4 of about 0.2, whereas the corrected power on 14 December varies in the main between −10 and 10 dB, corresponding to elevated values of S4 between 0.5 and 1.0. In particular, a close correspondence is found between the decrease in S4 from 12:30 to 14:00 UT on 14 December and the similar decrease in corrected radar power.

3 Conclusions

A close correspondence is found between the occurrence of elevated scintillation of transionospheric 250 MHz signals, quantified by the S4 index, and coherent backscatter power of a 10 MHz HF radar. The former is caused by F region ionospheric irregularities with scale sizes in the range of 100 m to 1 km; the latter by F region field-aligned irregularities with wavelengths of ∼15 m. This suggests that irregularities on a variety of scale sizes coexist at high latitudes.

The spatial-imaging capability of the radar shows that periods of low scintillation are associated with times when the auroral oval is located away from the ionospheric intersection point of the scintillation measurements, and high scintillation corresponds to times when the auroral oval coincides with it. That is, low scintillation at the intersection point is not an indication that scintillation is everywhere low. We hope in future to perform a more statistical comparison of coherent backscatter and scintillation. This will allow us to investigate the spectral width of the backscatter with the spectral width of the scintillation spectra, which might also be expected to correlate.

Acknowledgements. Topical Editor M. Pinnock thanks M. Keskinen and another referee for their help in evaluating this paper – SEM was supported by PPARC grant no. PPA/N/S/2000/00197. The work at AFRL and BC are partially supported by AFOSR Task 2311AS.

References

Basu, S., Basu, Su., Aarons, J., McClure, J. P., and Cousins, M. D.: On the coexistence of kilometre and meter scale irregularities in the nighttime equatorial F-region, J. Geophys. Res., 53, 4219–4226, 1978.

Basu, Su., Basu, S., MacKenzie, E., Fougere, P. F., Coley, W. R., Maynard, N. C., Winningham, J. D., Sugiura, M., Hanson, W.

B., and Hoegy, W. R.: Simultaneous density and electric field fluctuation spectra associated with velocity shear in the auroral oval, J. Geophys. Res., 93, 115–136, 1988.

Basu, S. and Basu, Su.: Ionospheric structures and scintillation spectra, in Wave Propagation in Random Media (Scintillation), edited by V .I. Tatarskii, A. Ishimaru and V. U. Zavortny, SPIE, Washington, DC, 139–155, 1993.

Basu, S., Weber, E. J., Bullett, T. W., Keskinen, M. J., MacKenzie, E., Doherty, P., Sheehan, R., Kuenzler, H., Ning, P., and Bongiolatti, J.: Characteristics of plasma structuring in the cusp/cleft region at Svalbard, Radio Sci., 33, 1885–1899, 1998.

Feldstein, Y. I. and Starkov, G. V.: Dynamics of auroral belt and polar geomagnetic disturbances, Planet. Space Sci., 15, 209–230, 1967.

Hall, G. E., MacDougall, J. W., Moorcroft, D. R., St.-Maurice, J.-P., Manson, A. H., and Meek, C. E.: Super Dual Auroral Radar Network observations of meteor echoes, J. Geophys. Res., 102, 14 603, 1997.

Lester, M., Chapman, P. J., Cowley, S. W. H., Crooks, S., Davies, J. A., McWillaims, K. A., Milan, S. E., Parsons, M., Payne, D., Thomas, E. C., Thornhill, J., Wade, N. M., Yeoman, T. K., and Barnes, R. J.: Stereo-CUTLASS A new capability of the SuperDARN HF radars, Ann. Geophys., 22, 459–473, 2004,
SRef-ID: 1432-0576/ag/2004-22-459.

Milan, S. E., Davies, J. A., and Lester, M.: Coherent HF radar backscatter characteristics associated with auroral forms identified by incoherent radar techniques: a comparison of CUTLASS and EISCAT observations, J. Geophys. Res., 104, 22 591–22 604, 1999.

Milan, S. E., Lester, M., Cowley, S. W. H., Oksavik, K., Brittnacher, M., Greenwald, R. A., Sofko, G., and Villain, J.-P.: Variations in polar cap area during two substorm cycles, Ann. Geophys., 21, 1121–1140, 2003,
SRef-ID: 1432-0576/ag/2003-21-1121.

Milan, S. E., Yeoman, T. K., Lester, M., Thomas, E. C., and Jones, T. B.: Initial backscatter occurrence statistics from the CUTLASS HF radars, Ann. Geophys., 15, 703–718, 1997,
SRef-ID: 1432-0576/ag/1997-15-703.

Milan, S. E., Yeoman, T. K., and Lester, M.: The dayside auroral zone as a hard target for coherent HF radars, Geophys. Res. Lett., 25, 3717–3720, 1998.

Tsunoda, R. T.: High latitude F region irregularities: A review and synthesis, Rev. Geophys., 26, 719–60, 1988.

Woodman, R. F. and Basu, Su.: Comparison between in situ spectral measurements of equatorial F region irregularities and backscatter observations at 3-m wavelength, Geophys. Res. Lett., 5, 869–872, 1978.

Yeoman, T. K., Wright, D. M., Stocker, A. J., and Jones, T. B.: An evaluation of range accuracy in the SuperDARN over-the-horizon HF radar systems, Radio Sci., 36, 801–813, 2001.